

# Description of single- $\Lambda$ hypernuclei with a relativistic point-coupling model

Y. Tanimura and K. Hagino

*Department of Physics, Tohoku University, Sendai 980-8578, Japan*

(Received 6 November 2011; revised manuscript received 15 December 2011; published 9 January 2012)

We extend the relativistic point-coupling model to single- $\Lambda$  hypernuclei. For this purpose, we add  $N$ - $\Lambda$  effective contact couplings to the model Lagrangian and determine the parameters by fitting to the experimental data for  $\Lambda$  binding energies. Our model well reproduces the data over a wide range of mass region although some of our interactions yield the reverse ordering of the spin-orbit partners from that of nucleons for heavy hypernuclei. The consistency of the interaction with the quark model predictions is also discussed.

DOI: [10.1103/PhysRevC.85.014306](https://doi.org/10.1103/PhysRevC.85.014306)

PACS number(s): 21.80.+a, 23.20.Lv, 21.30.Fe, 21.60.Jz

## I. INTRODUCTION

Relativistic mean-field (RMF) theory has been successfully applied to both finite nuclei and nuclear matter to describe their bulk properties [1–5]. Starting from an effective Lagrangian in which nucleon and meson fields are coupled in a covariant manner, single-particle Dirac equations for nucleons are derived within the mean-field approximation. In this model, nucleons are treated as Dirac particles moving independently in the mean field generated by the mesons. The spin-orbit interaction with the correct sign and magnitude naturally arises from the relativistic treatment of nucleons. The success of the model affirms the meson exchange picture of a nucleon-nucleon interaction in nuclei.

Recently, another class of relativistic model, that is, the relativistic point-coupling (RPC) model [6,7] has also been widely employed [8–14]. This model consists of Skyrme-type zero-range interactions and has been found to be as capable as meson exchange RMF models of reproducing the properties of finite nuclei and nuclear matter [7,8,11–13]. This model has several advantages compared to the meson exchange models. First, there is no need to solve the Klein-Gordon equations for mesons since the mesonic degrees of freedom are all implicit in the RPC model. Second, the Fock terms can easily be introduced by using the Fierz transformation because of its zero-range nature [9,10]. Last, it is much easier to apply the model to beyond-mean-field methods such as the generator coordinate method (GCM), and angular momentum and particle number projections [12,13].

A zero-range-type interaction is suitable also for the three-dimensional (3D) mesh method for mean-field calculations in the coordinate space representation [15,16]. With this method, an arbitrary deformation of nuclei can be efficiently described, and the method has been widely used in nonrelativistic Skyrme Hartree-Fock (SHF) calculations together with the imaginary time technique [15,16]. An extension of this method to the relativistic approach is not trivial, however. That is, a naive imaginary time evolution breaks down in relativistic systems due to the presence of the Dirac sea [17,18]. This is not a numerical, but rather a fundamental problem related to the variational principle. Such phenomena have been well-known under the name of “variational collapse” in the field of relativistic quantum chemistry [19–23]. For this reason, a 3D mesh calculation has not yet been carried out with either RMF or RPC. Recently, a few prescriptions to avoid the

variational collapse have been tested in the nuclear physics context [17,18]. The prescriptions were found to work well, at least for simple spherical systems, and a 3D mesh calculation may now be almost ready to perform.

In this paper, we extend the RPC model to hypernuclei. Effects of adding a  $\Lambda$  particle on the shape of nuclei, that is, the glue-like role, are attracting much attention theoretically and experimentally [24–30]. The RMF theory with meson exchange model has been extended to hypernuclei to describe such effects by adding ordinary scalar and vector couplings of a  $\Lambda$  particle to  $\sigma$  and  $\omega$  mesons, respectively [24,25,31–44]. The authors of Refs. [31,32] fitted the coupling constants in the strange sector to the experimental data of  $\Lambda$  binding energies. In these calculations, the tensor coupling to the  $\omega$  meson, which is predicted by the quark model [33,34] to be much stronger for  $\Lambda$  than for nucleon, was also included to reproduce rather small  $\Lambda$  spin-orbit splittings. Our aim in this paper is to propose a zero-range version of the phenomenological RMF models for hypernuclei.

The paper is organized as follows. In Sec. II, we introduce the model Lagrangian for a point-coupling model extended to single- $\Lambda$  hypernuclei. In Sec. III, the optimal parameter set is obtained by fitting to experimental single-particle energies for the  $\Lambda$  particle. We also test its predictive power and a consistency with the quark model. In Sec. IV, we summarize the paper.

## II. MODEL

Our model Lagrangian for single- $\Lambda$  hypernuclei is given by

$$\mathcal{L} = \mathcal{L}_{\text{free}} + \mathcal{L}_{\text{em}} + \mathcal{L}_{\text{int}}^{NN} + \mathcal{L}_{\text{int}}^{N\Lambda}, \quad (1)$$

in which the free and electromagnetic parts are given by

$$\mathcal{L}_{\text{free}} = \bar{\psi}_N(i\partial - m_N)\psi_N + \bar{\psi}_\Lambda(i\partial - m_\Lambda)\psi_\Lambda, \quad (2)$$

$$\mathcal{L}_{\text{em}} = -e\bar{\psi}_N \not{A} \frac{1 - \tau_3}{2} \psi_N - \frac{1}{4} F_{\mu\nu} F^{\mu\nu}, \quad (3)$$

respectively. Here,  $\psi_N$ ,  $\psi_\Lambda$ , and  $A^\mu$  are the nucleon,  $\Lambda$ , and electromagnetic fields, respectively.  $F^{\mu\nu} = \partial^\mu A^\nu - \partial^\nu A^\mu$  is the electromagnetic field strength tensor. The masses of nucleon and  $\Lambda$  are denoted by  $m_N$  and  $m_\Lambda$ , respectively.  $\tau_3$  is the isospin matrix.

The RPC model for normal nuclei consists of four-fermion point couplings  $\mathcal{L}_{4f}$ , derivative terms  $\mathcal{L}_{\text{der}}$ , and higher-order terms  $\mathcal{L}_{\text{hot}}$  [8]. Here  $\mathcal{L}_{4f}$  is the leading order of zero-range approximation to the meson exchange interaction.  $\mathcal{L}_{\text{der}}$  simulates the finite ranges of the meson exchanges.  $\mathcal{L}_{\text{hot}}$  corresponds to the self-couplings of the scalar and vector mesons, which introduce a density dependence into  $N$ - $N$  contact couplings. These terms are given by

$$\mathcal{L}_{\text{int}}^{NN} = \mathcal{L}_{4f}^{NN} + \mathcal{L}_{\text{der}}^{NN} + \mathcal{L}_{\text{hot}}^{NN}, \quad (4)$$

with

$$\begin{aligned} \mathcal{L}_{4f}^{NN} = & -\frac{1}{2}\alpha_S(\bar{\psi}_N\psi_N)(\bar{\psi}_N\psi_N) \\ & -\frac{1}{2}\alpha_V(\bar{\psi}_N\gamma_\mu\psi_N)(\bar{\psi}_N\gamma^\mu\psi_N) \\ & -\frac{1}{2}\alpha_{TS}(\bar{\psi}_N\vec{\tau}\psi_N) \cdot (\bar{\psi}_N\vec{\tau}\psi_N) \\ & -\frac{1}{2}\alpha_{TV}(\bar{\psi}_N\gamma_\mu\vec{\tau}\psi_N) \cdot (\bar{\psi}_N\gamma^\mu\vec{\tau}\psi_N), \end{aligned} \quad (5)$$

$$\begin{aligned} \mathcal{L}_{\text{der}}^{NN} = & -\frac{1}{2}\delta_S(\partial_\mu\bar{\psi}_N\psi_N)(\partial^\mu\bar{\psi}_N\psi_N) \\ & -\frac{1}{2}\delta_V(\partial_\mu\bar{\psi}_N\gamma_\nu\psi_N)(\partial^\mu\bar{\psi}_N\gamma^\nu\psi_N) \\ & -\frac{1}{2}\delta_{TS}(\partial_\mu\bar{\psi}_N\vec{\tau}\psi_N) \cdot (\partial^\mu\bar{\psi}_N\vec{\tau}\psi_N) \\ & -\frac{1}{2}\delta_{TV}(\partial_\mu\bar{\psi}_N\gamma_\nu\vec{\tau}\psi_N) \cdot (\partial^\mu\bar{\psi}_N\gamma^\nu\vec{\tau}\psi_N), \end{aligned} \quad (6)$$

and

$$\begin{aligned} \mathcal{L}_{\text{hot}}^{NN} = & -\frac{1}{3}\beta_S(\bar{\psi}_N\psi_N)^3 - \frac{1}{4}\gamma_S(\bar{\psi}_N\psi_N)^4 \\ & -\frac{1}{4}\gamma_V[(\bar{\psi}_N\gamma_\mu\psi_N)(\bar{\psi}_N\gamma^\mu\psi_N)]^2. \end{aligned} \quad (7)$$

Notice that the four different spin-isospin vertex structures labeled by the subscripts  $S$ ,  $V$ ,  $TS$ , and  $TV$  in the coupling constants correspond to  $\sigma$ ,  $\omega$ ,  $\delta$ , and  $\rho$  meson exchanges, respectively. Thus, we can find one-to-one correspondence of each term to the meson exchange model.

Noticing that  $\Lambda$  only couples to the scalar and vector mesons, we construct  $N$ - $\Lambda$  interaction as

$$\mathcal{L}_{\text{int}}^{N\Lambda} = \mathcal{L}_{4f}^{N\Lambda} + \mathcal{L}_{\text{der}}^{N\Lambda} + \mathcal{L}_{\text{ten}}^{N\Lambda}, \quad (8)$$

where

$$\begin{aligned} \mathcal{L}_{4f}^{N\Lambda} = & -\alpha_S^{(N\Lambda)}(\bar{\psi}_N\psi_N)(\bar{\psi}_\Lambda\psi_\Lambda) \\ & -\alpha_V^{(N\Lambda)}(\bar{\psi}_N\gamma_\mu\psi_N)(\bar{\psi}_\Lambda\gamma^\mu\psi_\Lambda), \end{aligned} \quad (9)$$

$$\begin{aligned} \mathcal{L}_{\text{der}}^{N\Lambda} = & -\delta_S^{(N\Lambda)}(\partial_\mu\bar{\psi}_N\psi_N)(\partial^\mu\bar{\psi}_\Lambda\psi_\Lambda) \\ & -\delta_V^{(N\Lambda)}(\partial_\mu\bar{\psi}_N\gamma_\nu\psi_N)(\partial^\mu\bar{\psi}_\Lambda\gamma^\nu\psi_\Lambda), \end{aligned} \quad (10)$$

and

$$\mathcal{L}_{\text{ten}}^{N\Lambda} = \alpha_T^{(N\Lambda)}(\bar{\psi}_\Lambda\sigma^{\mu\nu}\psi_\Lambda)(\partial_\nu\bar{\psi}_N\gamma_\mu\psi_N). \quad (11)$$

For simplicity, we do not consider the higher-order term for the  $N\Lambda$  coupling,  $\mathcal{L}_{\text{hot}}^{N\Lambda}$ , in this paper.  $\mathcal{L}_{\text{ten}}^{N\Lambda}$  in Eq. (11) simulates the  $\Lambda$ - $\omega$  tensor coupling  $\mathcal{L}_{\text{ten}}^{\Lambda\omega} = \frac{f_{\Lambda\omega}}{2m_\Lambda}(\bar{\psi}_\Lambda\sigma^{\mu\nu}\psi_\Lambda)(\partial_\nu\omega_\mu)$ . As we mentioned in the introduction, the quark model suggests that the tensor coupling of  $\Lambda$  to  $\omega$  meson is much stronger than that of nucleon. That is, the quark model yields the ratio of  $\Lambda$ - $\omega$  tensor-to-vector coupling constants,  $f_{\Lambda\omega}/g_{\Lambda\omega}$ , to be  $-1$ , while it yields the corresponding ratio for nucleon to be  $f_{N\omega}/g_{N\omega} = -0.09$  [33]. Thus, this type of coupling plays an important role in hypernuclei. Because this term is proportional to the derivative of the mean field, it mainly affects the spin-orbit splittings of  $\Lambda$  single-particle energies [31]. It is expected that the small spin-orbit splittings of  $\Lambda$  can be reproduced by tuning the tensor coupling  $\alpha_T^{(N\Lambda)}$ . We discuss this point in the next section.

Our model presented in this paper is similar to the one adopted in Ref. [35] by Finelli *et al.*, which is based on the chiral SU(3) dynamics. The  $N$ - $\Lambda$  part of their model consists of the density-dependent contact four fermion couplings of the scalar and the vector types, as well as the derivative term of the scalar type. A part of the four fermion terms effectively describes unresolved short-distance physics, while the density dependence is attributed to in-medium Nambu-Goldstone boson (two-pion and kaon) exchanges. The coefficients for the density dependence are fixed by the chiral SU(3) perturbation theory. The tensor interaction caused by  $2\pi$  exchange is treated in the model of Ref. [35] as first-order perturbation on the Hartree single-particle energies. In contrast to the model of Finelli *et al.*, we determine all the parameters phenomenologically, and thus we consider in our model also the derivative coupling of the vector type, which is absent in theirs.

The total energy corresponding to the Lagrangian in Eq. (1) for a single- $\Lambda$  hypernucleus with mass number  $A$  (i.e., a single  $\Lambda$  particle with  $A-1$  nucleons) in the mean-field (Hartree) and the no-sea approximations is given by

$$\begin{aligned} E = & \int d^3r \left( \sum_{i=1}^{A-1} \psi_i^\dagger(\vec{\alpha} \cdot \vec{p} + m_N\beta)\psi_i + \psi_\Lambda^\dagger(\vec{\alpha} \cdot \vec{p} + m_\Lambda\beta)\psi_\Lambda + \frac{1}{2}eA^0\rho_V^{(p)} + \frac{1}{2}\sum_K\alpha_K\rho_K^2 + \frac{1}{2}\sum_K\delta_K\rho_K\Delta\rho_K \right. \\ & \left. + \frac{1}{3}\beta_S\rho_S^3 + \frac{1}{4}\gamma_S\rho_S^4 + \frac{1}{4}\gamma_V\rho_V^4 + \sum_{K=S,V}\alpha_K^{(N\Lambda)}\rho_K\rho_K^{(\Lambda)} + \sum_{K=S,V}\delta_K^{(N\Lambda)}\rho_K\Delta\rho_K^{(\Lambda)} + \alpha_T^{(N\Lambda)}\rho_T^{(\Lambda)}\rho_V \right), \end{aligned} \quad (12)$$

where  $\vec{\alpha}$  and  $\beta$  are the usual Dirac matrices. Here we have assumed the time-reversal invariance of the nuclear ground state. The densities appearing in Eq. (12) are defined as

$$\rho_S = \sum_{i=1}^{A-1}\bar{\psi}_i\psi_i, \quad \rho_V = \sum_{i=1}^{A-1}\psi_i^\dagger\psi_i, \quad (13)$$

$$\rho_{TS} = \sum_{i=1}^{A-1}\bar{\psi}_i\tau_3\psi_i, \quad \rho_{TV} = \sum_{i=1}^{A-1}\psi_i^\dagger\tau_3\psi_i, \quad (14)$$

$$\rho_S^{(\Lambda)} = \bar{\psi}_\Lambda\psi_\Lambda, \quad \rho_V^{(\Lambda)} = \psi_\Lambda^\dagger\psi_\Lambda, \quad (15)$$

$$\rho_T^{(\Lambda)} = \vec{\nabla} \cdot (\bar{\psi}_\Lambda i\vec{\alpha}\psi_\Lambda). \quad (16)$$

Here  $\psi_i$  is the wave function for the  $i$ th nucleon, and  $\psi_\Lambda$  is the wave function for the  $\Lambda$  particle.

The relativistic Hartree equations for the nucleons and  $\Lambda$  particle are obtained by taking the variation of the energy with respect to the wave functions as

$$\frac{\delta}{\delta\psi_i^\dagger(\vec{r})} \left( E - \sum_{j=1}^A \epsilon_j \int d^3r' \psi_j^\dagger \psi_j \right) = 0, \quad (17)$$

where  $\epsilon_i$  is a Lagrange multiplier which ensures the normalization of the single-particle wave functions. Variation with respect to the nucleon wave function leads to the Hartree equation for nucleons,

$$[\vec{\alpha} \cdot \vec{p} + V_V + V_{TV} \tau_3 + V_C + (m_N + V_S + V_{TS} \tau_3) \beta] \psi_i = \epsilon_i \psi_i, \quad (18)$$

with

$$\begin{aligned} V_S &= \alpha_S \rho_S + \beta_S \rho_S^2 + \gamma_S \rho_S^3 + \delta_S \Delta \rho_S \\ &\quad + \alpha_S^{(N\Lambda)} \rho_S^{(\Lambda)} + \delta_S^{(N\Lambda)} \Delta \rho_S^{(\Lambda)}, \\ V_V &= \alpha_V \rho_V + \gamma_V \rho_V^3 + \delta_V \Delta \rho_V \\ &\quad + \alpha_V^{(N\Lambda)} \rho_V^{(\Lambda)} + \delta_V^{(N\Lambda)} \Delta \rho_V^{(\Lambda)} + \alpha_T^{(N\Lambda)} \rho_T^{(\Lambda)}, \\ V_{TS} &= \alpha_{TS} \rho_{TS} + \delta_{TS} \Delta \rho_{TS}, \\ V_{TV} &= \alpha_{TV} \rho_{TV} + \delta_{TV} \Delta \rho_{TV}, \\ V_C &= eA^0 \frac{1 - \tau_3}{2}, \quad (\Delta A^0 = -e\rho_V^{(p)}), \end{aligned} \quad (19)$$

while variation with respect to the  $\Lambda$  wave function leads to the Hartree equation for the  $\Lambda$  particle:

$$[\vec{\alpha} \cdot \vec{p} + U_V + U_T + (m_\Lambda + U_S) \beta] \psi_\Lambda = \epsilon_\Lambda \psi_\Lambda, \quad (20)$$

with

$$\begin{aligned} U_S &= \alpha_S^{(N\Lambda)} \rho_S + \delta_S^{(N\Lambda)} \Delta \rho_S, \\ U_V &= \alpha_V^{(N\Lambda)} \rho_V + \delta_V^{(N\Lambda)} \Delta \rho_V, \\ U_T &= -i\alpha_T^{(N\Lambda)} \beta \vec{\alpha} \cdot (\vec{\nabla} \rho_V). \end{aligned} \quad (21)$$

After having solved these Hartree equations self-consistently, we obtain the total binding energy as

$$\begin{aligned} E_B &= \sum_{i=1}^{A-1} \epsilon_i + \epsilon_\Lambda - E_{CM} - (A-1)m_N - m_\Lambda \\ &\quad - \int d^3r \left( \frac{1}{2} \sum_K \alpha_K \rho_K^2 + \frac{1}{2} \sum_K \delta_K \rho_K \Delta \rho_K \right. \\ &\quad + \frac{2}{3} \beta_S \rho_S^3 + \frac{3}{4} \gamma_S \rho_S^4 + \frac{3}{4} \gamma_V \rho_V^4 \\ &\quad + \sum_{K=S,V} \alpha_K^{(N\Lambda)} \rho_K \rho_K^{(\Lambda)} + \sum_{K=S,V} \delta_K^{(N\Lambda)} \rho_K \Delta \rho_K^{(\Lambda)} \\ &\quad \left. + \alpha_T^{(N\Lambda)} \rho_T^{(\Lambda)} \rho_V + \frac{1}{2} eA^0 \rho_V^{(p)} \right), \end{aligned} \quad (22)$$

where the center-of-mass energy  $E_{CM}$  is calculated by taking the expectation value of the kinetic energy for the center-of-mass motion with respect to the many-body ground state wave

function as

$$E_{CM} = \frac{\langle P_{CM}^2 \rangle}{2[(A-1)m_N + m_\Lambda]}. \quad (23)$$

See the Appendix for the explicit expression for this term.

The relation of the point-coupling model to the meson exchange model can be made as follows (see also Eqs. (6)–(10) in Ref. [8]). By eliminating the meson fields and expanding the meson propagators to the leading order, the following approximate relations between the two models can be obtained [8]:

$$\alpha_S \approx -\frac{g_{N\sigma}^2}{m_\sigma^2}, \quad \alpha_V \approx \frac{g_{N\omega}^2}{m_\omega^2}, \quad (24)$$

$$\alpha_S^{(N\Lambda)} \approx -\frac{g_{N\sigma} g_{\Lambda\sigma}}{m_\sigma^2}, \quad \alpha_V^{(N\Lambda)} \approx \frac{g_{N\omega} g_{\Lambda\omega}}{m_\omega^2},$$

$$\alpha_T^{(N\Lambda)} \approx -\frac{g_{N\omega} f_{\Lambda\omega}}{2m_\Lambda m_\omega^2}, \quad (25)$$

where  $g$ 's and  $m$ 's are the baryon-meson coupling constants and the meson masses, respectively.  $f_{\Lambda\omega}$  is the  $\Lambda$ - $\omega$  tensor coupling constant. Notice that it has been demonstrated that  $\alpha_S$  and  $\alpha_V$  obtained phenomenologically approximately follow these relations [8] (on the other hand, it has been shown that the derivative terms,  $\delta_S$  and  $\delta_V$ , do not follow the corresponding expected relations [8], and we do not discuss them in this paper). If we assume the naive quark counting ratios  $g_{\Lambda\sigma} = \frac{2}{3}g_{N\sigma}$  and  $g_{\Lambda\omega} = \frac{2}{3}g_{N\omega}$ , together with the quark model prediction for the tensor coupling,  $f_{\Lambda\omega}/g_{\Lambda\omega} = -1$ , we obtain

$$\alpha_S^{(N\Lambda)} \approx \frac{2}{3}\alpha_S, \quad \alpha_V^{(N\Lambda)} \approx \frac{2}{3}\alpha_V, \quad \alpha_T^{(N\Lambda)} \approx -\frac{\alpha_V}{3m_\Lambda}. \quad (26)$$

We will show in the next section that these expected relations indeed hold if we include the  $N$ - $\Lambda$  tensor coupling given by Eq. (11) in the Lagrangian.

### III. RESULTS AND DISCUSSION

With the model described in the previous section, we calculate  $\Lambda$  binding energies defined by the mass difference

$$m^{(A-1)Z} + m_\Lambda - m_\Lambda^{(A)Z} = E_B^{(A-1)Z} - E_B^{(A)Z}. \quad (27)$$

To this end, we assume spherical symmetry, and neglect the pairing correlations for simplicity. For the valence orbit, we use the filling approximation to determine the occupation probability. We set the masses of baryons to  $m_N = 938$  MeV and  $m_\Lambda = 1115.6$  MeV. We use the parameter set PC-F1 [8] for the  $N$ - $N$  part of interaction and fit the five parameters in the  $N$ - $\Lambda$  part [see Eqs. (9)–(11)] to the experimental data. The data to be fitted to are  $\Lambda$  binding energies for  $s$  and  $p$  orbitals in  $^{16}_\Lambda\text{O}$ ,  $s$ ,  $p$ , and  $d$  in  $^{40}_\Lambda\text{Ca}$ ,  $s$  and  $d$  in  $^{51}_\Lambda\text{V}$ ,  $s$ ,  $p$ ,  $d$ , and  $f$  in  $^{89}_\Lambda\text{Y}$ ,  $s$ ,  $p$ ,  $d$ ,  $f$ , and  $g$  in  $^{139}_\Lambda\text{La}$ , and  $s$ ,  $p$ ,  $d$ ,  $f$ , and  $g$  in  $^{208}_\Lambda\text{Pb}$ . These are taken from Refs. [45,46]. In addition, the spin-orbit splitting for the  $p$  orbital of  $\Lambda$  in  $^{16}_\Lambda\text{O}$  [47] is included in the fitting procedure. The value deduced in Ref. [47] is  $300 \text{ keV} \leq \epsilon_{\Lambda p_{1/2}} - \epsilon_{\Lambda p_{3/2}} \leq 600 \text{ keV}$ , where the variation comes from a choice of the interactions. Notice that

TABLE I. The best fit parameter set PCY-S1 for the RPC model for hypernuclei. PC-F1 [8] is used for the  $N$ - $N$  part. The uncorrelated errors and the ratios  $R$  defined in Eq. (29) with the expected values given in Eq. (26) are also shown in the table. The  $\chi^2$  value per degree of freedom is  $\chi_{\text{dof}}^2 = 0.54$ .

Coupling constant	Value	Uncorrelated error (%)	$R$
$\alpha_S^{(NA)}$	$-2.0305 \times 10^{-4} \text{ MeV}^{-2}$	$8.2 \times 10^{-2}$	0.79
$\alpha_V^{(NA)}$	$1.6548 \times 10^{-4} \text{ MeV}^{-2}$	$9.7 \times 10^{-2}$	0.96
$\delta_S^{(NA)}$	$2.2929 \times 10^{-9} \text{ MeV}^{-4}$	$5.4 \times 10^{-1}$	–
$\delta_V^{(NA)}$	$-2.3872 \times 10^{-9} \text{ MeV}^{-4}$	$5.0 \times 10^{-1}$	–
$\alpha_T^{(NA)}$	$-1.0603 \times 10^{-7} \text{ MeV}^{-3}$	$6.8 \times 10^0$	1.37

this value is model dependent, and we merely regard it as a criterion. The coupling constants in the strange sector are determined by performing a least-squares fit to the data, that is, by minimizing the quantity

$$\chi^2 = \sum_{i=1}^N \left( \frac{O_i^{\text{theor}} - O_i^{\text{expt}}}{\Delta O_i^{\text{expt}}} \right)^2. \quad (28)$$

Here  $N$  is the number of data points, and  $O_i^{\text{theor}}$  and  $O_i^{\text{expt}}$  are theoretical and experimental values of the observables, respectively, with the experimental uncertainties of  $\Delta O_i^{\text{expt}}$ . To find the minimum of  $\chi^2$  in the 5D parameter space, we employ an automatic search algorithm *Oak Ridge and Oxford method* [48].

The parameter set PCY-S1 so obtained is summarized in Table I. We also show the uncorrelated errors for the parameters, which are defined as the range of a parameter that changes the  $\chi^2$  value by unity around the minimum value when the other parameters are kept to be the same. Together with the coupling constants and their uncorrelated errors, the ratios  $R$  of the resultant  $N$ - $\Lambda$  coupling constants to the expected values given in Eq. (26),

$$R = (\text{resulted value})/(\text{expected value}), \quad (29)$$

are also shown. These ratios are  $R = 0.79, 0.96$ , and  $1.37$  for  $\alpha_S^{(NA)}$ ,  $\alpha_V^{(NA)}$ , and  $\alpha_T^{(NA)}$ , respectively, and the expected values are approximately realized.

The calculated binding energies of  $\Lambda$  with this interaction are shown in Fig. 1(a). One observes that the calculated  $\Lambda$  binding energies agree with the experimental values fairly well, although the binding energies for  ${}_{\Lambda}^{28}\text{Si}$  and  ${}_{\Lambda}^{32}\text{S}$  are somewhat overestimated. The less satisfactory result for these latter nuclei, which has been observed also in the previous RMF calculations for hypernuclei [31,32,39,41], is within expectation as we do not take into account a strong deformation of the core nucleus nor the pairing correlation. We have confirmed that the situation does not change even if we include these two nuclei in the fitting.

To investigate the role of the tensor coupling, we show in Table II the parameter set PCY-S2 obtained *without* including the tensor coupling term. The  $\Lambda$  binding energies calculated with this interaction are shown in Fig. 2(a). As one sees, the agreement with the experimental data is worsened as compared to PCY-S1, and the ratios  $R$  are strongly suppressed compared

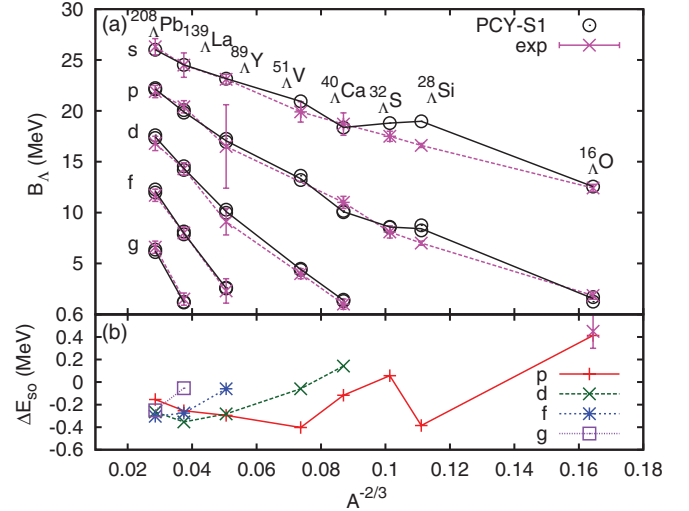


FIG. 1. (Color online) Comparison between the experimental data and the calculated  $\Lambda$  binding energies  $B_\Lambda$  [Fig. 1(a)] and spin-orbit splittings of  $\Lambda$  single-particle energies  $\Delta E_{\text{so}}$  [Fig. 1(b)] obtained with the parameter set PCY-S1. The experimental data are taken from Refs. [45–47].

to unity. On the other hand, the sum  $\alpha_S^{(NA)} + \alpha_V^{(NA)}$  has similar values around  $-3 \times 10^{-5} \text{ MeV}^{-2}$  for PCY-S1 and PCY-S2. The suppression of the ratios can be understood as follows. In the nonrelativistic reduction of a Dirac equation without the tensor coupling contribution, the central potential and the spin-orbit potential read

$$V_{\text{central}} = V + S, \quad V_{\text{is}} = \frac{1}{2m^2} \frac{1}{r} \frac{d}{dr} (V - S), \quad (30)$$

where  $V$  and  $S$  are the vector and the scalar potentials, respectively. Therefore, to reproduce a small spin-orbit splitting of  $\Lambda$  without the tensor interaction, the difference of the vector and the scalar potential have to be small, keeping their sum constant. This can be achieved only by lowering the values of the four fermion  $N$ - $\Lambda$  couplings,  $\alpha_S^{(NA)}$  and  $\alpha_V^{(NA)}$ , which roughly determine the strengths of mean potential felt by  $\Lambda$ . Notice that  $V - S$  does not have to be small in the presence of the tensor coupling, as there is another contribution to the spin-orbit potential from the tensor coupling. The importance of the  $N$ - $\Lambda$  tensor coupling (originated from the  $\Lambda$ - $\omega$  tensor coupling) is thus evident. It yields small spin-orbit splittings, keeping  $\alpha_S^{(NA)}$  and  $\alpha_V^{(NA)}$  at the natural values. In PCY-S1,

TABLE II. The parameter set PCY-S2 obtained by the omitting the tensor coupling.  $\chi_{\text{dof}}^2$  is 0.85.

Coupling constant	Value	Uncorrelated error (%)	$R$
$\alpha_S^{(NA)}$	$-4.2377 \times 10^{-5} \text{ MeV}^{-2}$	$3.6 \times 10^{-1}$	0.17
$\alpha_V^{(NA)}$	$1.4268 \times 10^{-5} \text{ MeV}^{-2}$	$1.0 \times 10^0$	0.08
$\delta_S^{(NA)}$	$1.2986 \times 10^{-9} \text{ MeV}^{-4}$	$8.3 \times 10^{-1}$	–
$\delta_V^{(NA)}$	$-1.3850 \times 10^{-9} \text{ MeV}^{-4}$	$7.4 \times 10^{-1}$	–
$\alpha_T^{(NA)}$	0	–	–



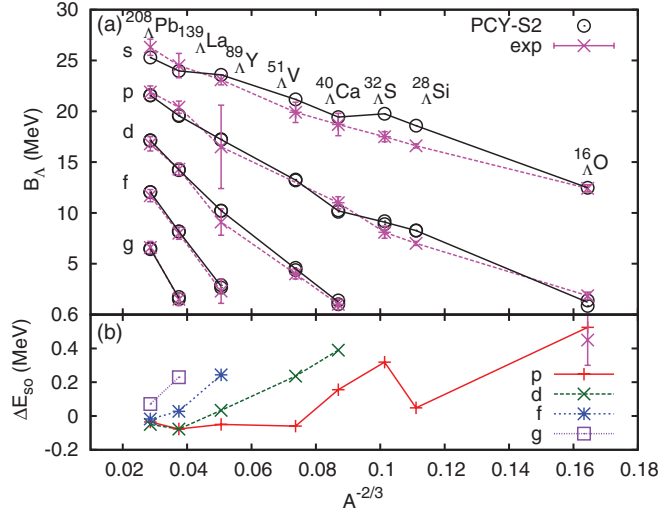


FIG. 2. (Color online) Same as Fig. 1, but with the parameter set PCY-S2.

the two predictions of the quark model, that is, the quark counting ratios and the importance of the tensor coupling ( $f_{\Lambda\omega}/g_{\Lambda\omega} = -1$ ), are simultaneously satisfied.

Let us now discuss the calculated spin-orbit splittings,  $\Delta E_{so}$ . These are estimated as a difference of  $\Lambda$  single-particle energies between spin-orbit partners,  $\Delta E_{so} = \epsilon_{\Lambda, j=l-1/2} - \epsilon_{\Lambda, j=l+1/2}$ , when the  $\Lambda$  particle is put in the lowest  $s$  orbital. Those obtained with PCY-S1 and PCY-S2 are shown in Figs. 1(b) and 2(b), respectively. For both the parameter sets, although the absolute values of  $\Delta E_{so}$  are smaller by roughly a factor of 10 than those for nucleon,  $\Delta E_{so}$  alters its sign depending on the mass number. Notice that the spin-orbit splittings may be inverted depending on the strength of the tensor coupling term, as one can see in Fig. 2 of Ref. [31]. One may consider this inversion somewhat ill favored. We mention, however, that at present there have been no experimental data which exclude the possible inversion of the spin-orbit splitting in the medium and heavier mass region.

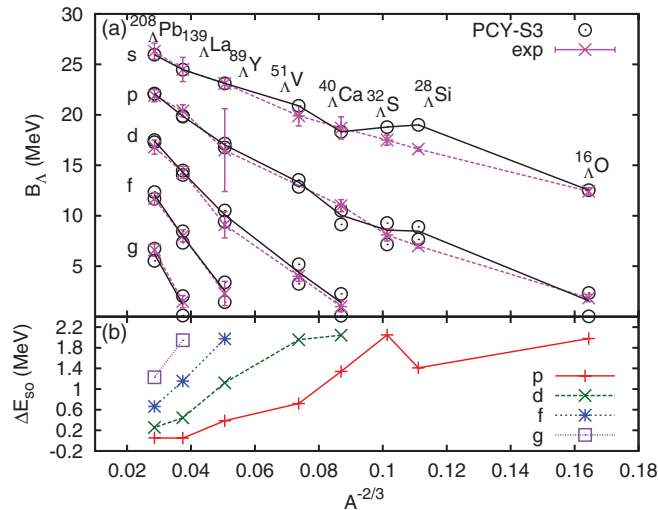


FIG. 3. (Color online) Same as Fig. 1, but with the parameter set PCY-S3.

TABLE III. The parameter set PCY-S3 obtained without fitting to the spin-orbit splitting in  $^{16}_{\Lambda}\text{O}$ .  $\chi^2_{\text{dof}}$  is 0.57.

Coupling constant	Value	Uncorrelated error (%)	$R$
$\alpha_S^{(N\Lambda)}$	$-2.0197 \times 10^{-4} \text{ MeV}^{-2}$	$7.4 \times 10^{-2}$	0.79
$\alpha_V^{(N\Lambda)}$	$1.6449 \times 10^{-4} \text{ MeV}^{-2}$	$9.1 \times 10^{-2}$	0.95
$\delta_S^{(N\Lambda)}$	$2.3514 \times 10^{-9} \text{ MeV}^{-4}$	$4.5 \times 10^{-1}$	–
$\delta_V^{(N\Lambda)}$	$-2.4993 \times 10^{-9} \text{ MeV}^{-4}$	$4.5 \times 10^{-1}$	–
$\alpha_T^{(N\Lambda)}$	$-4.0820 \times 10^{-9} \text{ MeV}^{-3}$	$5.5 \times 10^2$	0.05

If we exclude the spin-orbit splitting of the  $1p$  state of  $\Lambda$  in  $^{16}_{\Lambda}\text{O}$  from the fitting, that is, if we fit only the energy centroid of each spin-orbit partner, we obtain Fig. 3 for the  $\Lambda$  binding energies and the spin-orbit splittings. The parameters for this set, PCY-S3, are summarized in Table III. For this parameter set, the vector and scalar couplings of  $\Lambda$  to nucleon remain natural, but the tensor coupling is far smaller than the expected value in Eq. (26). Because there is no constraint on the value of spin-orbit splitting, this parameter set yields unacceptably large spin-orbit splitting, some of them stretching even beyond the experimental uncertainties (i.e., the upper bounds).

Last, we examine the role played by the derivative terms in the Lagrangian. In Ref. [49], it was pointed out that only one derivative term is well constrained by the bulk nuclear observables; that is, inclusion of a single derivative term is sufficient to obtain a good fit. Finelli *et al.* have shown that their model with only a scalar derivative coupling indeed reproduces well the data for normal nuclei [50] and hypernuclei [35]. For the same reason, Nikšić *et al.* [11] constructed their point-coupling interaction with only a single derivative coupling. Following Refs. [11,35,50], we construct another parameter set PCY-S4 by omitting the vector derivative term. The results are shown in Table IV and Fig. 4. One observes that the quality of the fit is as good as the other parameter sets. The agreement with the quark model prediction is also good, and the inversion of the spin-orbit partner is not seen for this force. Furthermore, we find that the spin-orbit splittings in the medium-mass region are relatively larger than those in the light- and the heavy-mass regions. This is in a similar trend as in the results of the meson exchange interaction PK1-Y1 [32]. Therefore, PCY-S4 provides an alternative parameter set to PCY-S1, where the main difference between the two interactions is whether the spin-orbit splitting is normal (PCY-S4) or inverted (PCY-S1).

TABLE IV. The parameter set PCY-S4 obtained by setting the vector derivative coupling,  $\delta_V^{(N\Lambda)}$ , to be zero.  $\chi^2_{\text{dof}}$  is 0.92.

Coupling constant	Value	Uncorrelated error (%)	$R$
$\alpha_S^{(N\Lambda)}$	$-1.8594 \times 10^{-4} \text{ MeV}^{-2}$	$8.7 \times 10^{-2}$	0.72
$\alpha_V^{(N\Lambda)}$	$1.4981 \times 10^{-4} \text{ MeV}^{-2}$	$1.0 \times 10^{-1}$	0.87
$\delta_S^{(N\Lambda)}$	$-1.9958 \times 10^{-10} \text{ MeV}^{-4}$	$6.1 \times 10^0$	–
$\delta_V^{(N\Lambda)}$	0	–	–
$\alpha_T^{(N\Lambda)}$	$-5.5322 \times 10^{-8} \text{ MeV}^{-3}$	$1.7 \times 10^1$	0.71

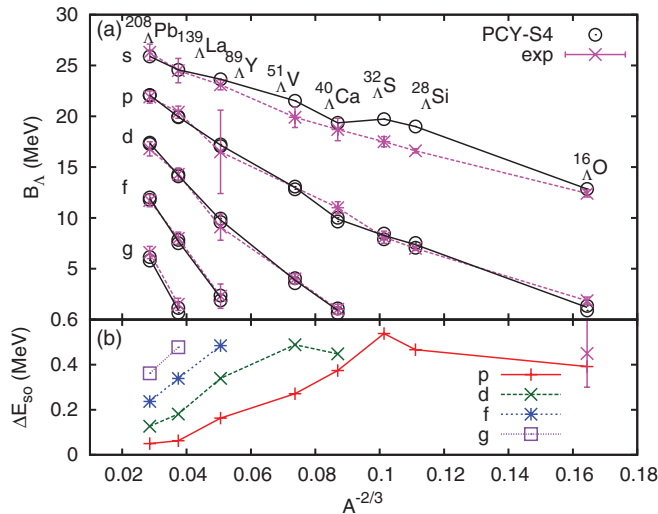


FIG. 4. (Color online) Same as Fig. 1, but with the parameter set PCY-S4.

#### IV. SUMMARY

We have proposed a new RPC model to describe single- $\Lambda$  hypernuclei in the mean-field approximation. This is a straightforward extension of the RPC model for nucleons, which has a similar structure as the Skyrme interaction. To this end, we added effective contact  $N$ - $\Lambda$  interactions, corresponding to the  $\Lambda$ - $\sigma$  and  $\Lambda$ - $\omega$  couplings, to the model Lagrangian. In addition, we introduced the zero-range  $N$ - $\Lambda$  tensor coupling as well to mimic the tensor coupling between  $\Lambda$  and  $\omega$  meson, following the quark model suggestion.

We fitted the coupling constants in the strange sector to the experimental data of  $\Lambda$  binding energies. The four parameter sets, PCY-S1, PCY-S2, PCY-S3, and PCY-S4 were proposed, which well reproduce the experimental data through the whole mass region. The resulting spin-orbit splittings in PCY-S1, PCY-S2, and PCY-S4 are smaller than that of nucleon by roughly a factor of 10 in their absolute values, although PCY-S3 yields too-large spin-orbit splittings. For PCY-S1 and PCY-S2 their signs are opposite that of nucleon in some nuclei in the heavier region. However, for PCY-S4 obtained without taking into account the vector derivative term, the sign of the spin-orbit splitting is the same as that for nucleons. High-precision  $\gamma$ -ray experiments for  $\Lambda$  single-particle energies are awaited to see whether the spin-orbit splitting of heavy hypernuclei is normal or inverted.

We have confirmed that the tensor coupling, which is ignored in the  $N$ - $N$  interaction, is quite important to reproduce the small spin-orbit splittings of  $\Lambda$  particle. Without the tensor coupling, the scalar and the vector couplings of  $\Lambda$  to nucleon are forced to be unnaturally weak (PCY-S2). The tensor coupling suppresses the spin-orbit splittings, keeping the scalar and the vector couplings consistent with the naive quark counting. The good consistency with the quark model found in our interaction can be a useful guide in further extending the point-coupling model to multi- $\Lambda$  or  $\Xi$  hypernuclei.

We conclude that the point-coupling model is capable of describing single- $\Lambda$  hypernuclei as well as normal nuclei. Many studies on hypernuclei have been carried out based on the finite range RMF models, for example, the halo phenomena [42], magnetic moment [43], and spin symmetry [44]. It would be interesting to explore whether the conclusions there remain the same with the zero-range RPC model proposed in this paper. The model can be an appropriate tool for relativistic calculations for hypernuclei on 3D mesh owing to its numerical simplicity. There has been no relativistic calculation performed on 3D mesh because of the variational difficulty. Thus, the primary future work is to develop an efficient calculation technique for relativistic calculations on 3D mesh that overcomes the “variational collapse.” A work in this direction is in progress. Further extensions of the point-coupling model to multi- $\Lambda$  and  $\Xi$  hypernuclei and an introduction of explicit density dependences into the coupling constants are also interesting future works.

#### ACKNOWLEDGMENTS

We thank H. Tamura, A. Ohnishi, J. A. Maruhn, and T. Koike for useful discussions. Discussions during the YIPQS international workshop at Yukawa Institute for Theoretical Physics, Kyoto University, on “Dynamics and Correlations in Exotic Nuclei 2011 (DCEN2011),” were useful to complete this work. This work was supported by the Global COE Program “Weaving Science Web beyond Particle-Matter Hierarchy” at Tohoku University and by the Japanese Ministry of Education, Culture, Sports, Science, and Technology by a Grant-in-Aid for Scientific Research under Program No. (C) 22540262.

#### APPENDIX: CENTER-OF-MASS ENERGY

In this Appendix, we give an explicit expression for the numerator of Eq. (23). Although it has already been given in Ref. [51], we have found a few typos in their expression for the relativistic case with spherical symmetry. Here we correct the typos and give the correct formula.

With the spherical symmetry, single-particle (s.p.) wave functions are given as

$$\psi_{\alpha m}(\vec{r}) = \begin{pmatrix} \psi_{\alpha}^{(+)}(r) \mathcal{Y}_{\ell_{\alpha}^{(+)} j_{\alpha} m}(\theta, \phi) \\ i \psi_{\alpha}^{(-)}(r) \mathcal{Y}_{\ell_{\alpha}^{(-)} j_{\alpha} m}(\theta, \phi) \end{pmatrix}, \quad (\text{A1})$$

where  $\alpha$  is a shorthand notation for  $\{n_{\alpha}, \ell_{\alpha}^{(+)}, j_{\alpha}\}$ , while  $m = j_z$ . Here  $n_{\alpha}$  is the principal quantum number,  $\ell_{\alpha}^{(+)}$  is the orbital angular momentum of the upper component of the s.p. spinor, and  $j_{\alpha}$  is the total angular momentum. The spherical spinor  $\mathcal{Y}_{\ell j m}$  is defined by  $\mathcal{Y}_{\ell j m} = \sum_{m' m''} \langle \ell m' \frac{1}{2} m'' | j m \rangle Y_{\ell m} \chi_{\frac{1}{2} m''}$ , where  $\chi_{\frac{1}{2} m''}$  is the spin-wave function. The orbital angular momentum of the lower component  $\ell_{\alpha}^{(-)}$  is given by  $\ell_{\alpha}^{(-)} = 2j_{\alpha} - \ell_{\alpha}^{(+)}$ . Following Ref. [51], we compute the center-of-mass correction in the nonrelativistic approximation. The expectation value of the squared center-of-mass momentum

$P_{\text{CM}}^2$  with a mean-field many-body state reads

$$\langle P_{\text{CM}}^2 \rangle = -\hbar^2 \sum_{\alpha} w_{\alpha} \sum_m \langle \psi_{\alpha m} | \Delta | \psi_{\alpha m} \rangle - \hbar^2 \sum_{\alpha, \beta} [w_{\alpha} w_{\beta} + \sqrt{w_{\alpha}(1-w_{\alpha})w_{\beta}(1-w_{\beta})}] \sum_{m, m'} |\langle \psi_{\alpha m} | \vec{\nabla} | \psi_{\beta m'} \rangle|^2, \quad (\text{A2})$$

with

$$\sum_m \langle \psi_{\alpha m} | \Delta | \psi_{\alpha m} \rangle = (2j_{\alpha} + 1) \sum_{\eta=\pm} \int dr r^2 \psi_{\alpha}^{(\eta)} \left[ \frac{\partial^2}{\partial r^2} + \frac{2}{r} \frac{\partial}{\partial r} - \frac{\ell_{\alpha}^{(\eta)}(\ell_{\alpha}^{(\eta)} + 1)}{r^2} \right] \psi_{\alpha}^{(\eta)}, \quad (\text{A3})$$

and

$$\begin{aligned} & \sum_{m, m'} |\langle \psi_{\alpha m} | \vec{\nabla} | \psi_{\beta m'} \rangle|^2 \\ &= (2j_{\alpha} + 1)(2j_{\beta} + 1) \sum_{\eta, \eta'} (-)^{\ell_{\alpha}^{(\eta)} + \ell_{\beta}^{(\eta')} + 1} \begin{Bmatrix} j_{\beta} & j_{\alpha} & 1 \\ \ell_{\alpha}^{(\eta)} & \ell_{\beta}^{(\eta')} & \frac{1}{2} \end{Bmatrix} \begin{Bmatrix} j_{\beta} & j_{\alpha} & 1 \\ \ell_{\alpha}^{(\eta')} & \ell_{\beta}^{(\eta)} & \frac{1}{2} \end{Bmatrix} \\ & \times \left[ \delta_{\ell_{\alpha}^{(\eta)}, \ell_{\beta}^{(\eta')} + 1} \sqrt{\ell_{\alpha}^{(\eta)}} \int dr r^2 \psi_{\alpha}^{(\eta)} \left( \frac{\partial}{\partial r} - \frac{\ell_{\beta}^{(\eta')}}{r} \right) \psi_{\beta}^{(\eta')} - \delta_{\ell_{\beta}^{(\eta)}, \ell_{\alpha}^{(\eta')} + 1} \sqrt{\ell_{\beta}^{(\eta)}} \int dr r^2 \psi_{\beta}^{(\eta)} \left( \frac{\partial}{\partial r} + \frac{\ell_{\alpha}^{(\eta')} + 1}{r} \right) \psi_{\alpha}^{(\eta')} \right] \\ & \times \left[ \delta_{\ell_{\beta}^{(\eta)}, \ell_{\alpha}^{(\eta')} + 1} \sqrt{\ell_{\beta}^{(\eta)}} \int dr r^2 \psi_{\beta}^{(\eta)} \left( \frac{\partial}{\partial r} - \frac{\ell_{\alpha}^{(\eta')}}{r} \right) \psi_{\alpha}^{(\eta')} - \delta_{\ell_{\alpha}^{(\eta)}, \ell_{\beta}^{(\eta')} + 1} \sqrt{\ell_{\alpha}^{(\eta)}} \int dr r^2 \psi_{\alpha}^{(\eta)} \left( \frac{\partial}{\partial r} + \frac{\ell_{\beta}^{(\eta')} + 1}{r} \right) \psi_{\beta}^{(\eta')} \right], \quad (\text{A4}) \end{aligned}$$

where  $w_{\alpha}$  is the occupation probability of the level  $\alpha$ .

- 
- [1] B. D. Serot and J. D. Walecka, *Adv. Nucl. Phys.* **16**, 1 (1986).  
[2] D. Vretenar, A. Afanasjev, G. A. Lalazissis, and P. Ring, *Phys. Rep.* **409**, 101 (2005).  
[3] P. Ring, *Prog. Part. Nucl. Phys.* **37**, 193 (1996).  
[4] J. Meng, H. Toki, S. G. Zhou, S. Q. Zhang, W. H. Long, and L. S. Geng, *Prog. Part. Nucl. Phys.* **57**, 470 (2006).  
[5] J. Boguta and A. R. Bodmer, *Nucl. Phys. A* **292**, 413 (1977).  
[6] P. Manakos and T. Mannel, *Z. Phys. A* **330**, 223 (1988).  
[7] B. A. Nikolaus, T. Hoch, and D. G. Madland, *Phys. Rev. C* **46**, 1757 (1992).  
[8] T. Bürvenich, D. G. Madland, J. A. Maruhn, and P.-G. Reinhard, *Phys. Rev. C* **65**, 044308 (2002).  
[9] J. A. Maruhn, T. Bürvenich, and D. G. Madland, *J. Comput. Phys.* **169**, 238 (2001).  
[10] A. Sulaksono, T. Bürvenich, J. A. Maruhn, P.-G. Reinhard, and W. Greiner, *Ann. Phys. (NY)* **306**, 36 (2003).  
[11] T. Nikšić, D. Vretenar, and P. Ring, *Phys. Rev. C* **78**, 034318 (2008).  
[12] J. M. Yao, J. Meng, P. Ring, and D. Vretenar, *Phys. Rev. C* **81**, 044311 (2010).  
[13] T. Nikšić, D. Vretenar, and P. Ring, *Phys. Rev. C* **73**, 034308 (2006); **74**, 064309 (2006); T. Nikšić, Z. P. Li, D. Vretenar, L. Próchniak, J. Meng, and P. Ring, *ibid.* **79**, 034303 (2009).  
[14] P. W. Zhao, Z. P. Li, J. M. Yao, and J. Meng, *Phys. Rev. C* **82**, 054319 (2010).  
[15] P. Bonche, H. Flocard, P.-H. Heenen, S. J. Krieger, and M. S. Weiss, *Nucl. Phys. A* **443**, 39 (1985).  
[16] P. Bonche, H. Flocard, and P.-H. Heenen, *Comput. Phys. Commun.* **171**, 49 (2005).  
[17] Y. Zhang, H. Liang, and J. Meng, *Int. J. Mod. Phys. E* **19**, 55 (2010).  
[18] K. Hagino and Y. Tanimura, *Phys. Rev. C* **82**, 057301 (2010).  
[19] H. Wallmeier and W. Kutzelnigg, *Chem. Phys. Lett.* **78**, 341 (1981).  
[20] H. Wallmeier and W. Kutzelnigg, *Phys. Rev. A* **28**, 3092 (1983).  
[21] R. E. Stanton and S. Havriliak, *J. Chem. Phys.* **81**, 1910 (1984).  
[22] R. N. Hill and C. Krauthausser, *Phys. Rev. Lett.* **72**, 2151 (1994).  
[23] P. Falsaperla, G. Fonte, and J. Z. Chen, *Phys. Rev. A* **56**, 1240 (1997).  
[24] M. T. Win and K. Hagino, *Phys. Rev. C* **78**, 054311 (2008).  
[25] B.-N. Lu, E.-G. Zhao, and S.-G. Zhou, *Phys. Rev. C* **84**, 014328 (2011).  
[26] M. T. Win, K. Hagino, and T. Koike, *Phys. Rev. C* **83**, 014301 (2011).  
[27] J. M. Yao, Z. P. Li, K. Hagino, M. Thi Win, Y. Zhang, and J. Meng, *Nucl. Phys. A* **868-869**, 12 (2011).  
[28] M. Isaka, M. Kimura, A. Dote, and A. Ohnishi, *Phys. Rev. C* **83**, 044323 (2011).  
[29] E. Hiyama, M. Kamimura, K. Miyazaki, and T. Motoba, *Phys. Rev. C* **59**, 2351 (1999).  
[30] K. Tanida *et al.*, *Phys. Rev. Lett.* **86**, 1982 (2001).  
[31] Y. Sugahara and H. Toki, *Prog. Theor. Phys.* **92**, 803 (1994).  
[32] C. Y. Song, J. M. Yao, H. F. Lü, and J. Meng, *Int. J. Mod. Phys. E* **19**, 2538 (2010).  
[33] J. Cohen and H. J. Weber, *Phys. Rev. C* **44**, 1181 (1991).  
[34] B. K. Jennings, *Phys. Lett. B* **246**, 325 (1990); M. Chiapparini, A. O. Gattone, and B. K. Jennings, *Nucl. Phys. A* **529**, 589 (1991).  
[35] P. Finelli, N. Kaiser, D. Vretenar, and W. Weise, *Nucl. Phys. A* **831**, 163 (2009); P. Finelli, *ibid.* **835**, 418 (2010).  
[36] R. Brockmann and W. Weise, *Phys. Lett. B* **69**, 167 (1977).  
[37] J. Boguta and S. Bohrmann, *Phys. Lett. B* **102**, 93 (1981).  
[38] A. Bouyssy, *Nucl. Phys. A* **381**, 445 (1982).  
[39] J. Mareš and B. K. Jennings, *Phys. Rev. C* **49**, 2472 (1994).  
[40] D. Vretenar, W. Pöschl, G. A. Lalazissis, and P. Ring, *Phys. Rev. C* **57**, R1060 (1998).  
[41] K. Tsubakihara, H. Maekawa, H. Matsumiya, and A. Ohnishi, *Phys. Rev. C* **81**, 065206 (2010).

- [42] H-F. Lü and J. Meng, *Chin. Phys. Lett.* **19**, 1775 (2002).
- [43] J-M. Yao, H-F. Lü, G. Hillhouse, and J. Meng, *Chin. Phys. Lett.* **25**, 1629 (2008).
- [44] C-Y. Song, J-M. Yao, and J. Meng, *Chin. Phys. Lett.* **26**, 122102 (2009).
- [45] O. Hashimoto and H. Tamura, *Prog. Part. Nucl. Phys.* **57**, 564 (2006).
- [46] Q. N. Usmani and A. R. Bodmer, *Phys. Rev. C* **60**, 055215 (1999).
- [47] T. Motoba, *Nucl. Phys. A* **639**, 135c (1998).
- [48] B. Alder, S. Fernbach, and M. Rotenberg, *Methods in Computational Physics*, Vol. 6 (Academic Press, New York and London, 1966).
- [49] R. J. Furnstahl and B. D. Serot, *Nucl. Phys. A* **671**, 447 (2000).
- [50] P. Finelli, N. Kaiser, D. Vretener, and W. Weise, *Nucl. Phys. A* **770**, 1 (2006).
- [51] M. Bender, K. Rutz, P.-G. Reinhard, and J. A. Maruhn, *Eur. Phys. J. A* **7**, 467 (2000).